

# Contraction in Human Myometrium Is Associated with Changes in Small Heat Shock Proteins

David A. MacIntyre, Elisa K. Tyson, Mark Read, Roger Smith, George Yeo, Kenneth Kwek, and Eng-Cheng Chan

Mothers and Babies Research Centre (D.A.M., E.K.T., M.R., R.S., E.-C.C.), The University of Newcastle, John Hunter Hospital, New Lambton Heights, Newcastle 2305, Australia; and KK Women's and Children's Hospital (G.Y., K.K.), Singapore 229899, Singapore

The myometrium undergoes substantial remodeling at the time of labor including rearrangement of the cellular contractile machinery. The regulation of this process in human myometrium at the time of labor is poorly defined, but evidence in other muscle types suggests modulation by small heat shock proteins (sHSP). The aim of this study was to investigate whether similar changes in sHSP occur in the myometrium at labor. Using a quantitative proteomic approach (two-dimensional difference gel electrophoresis), we found a 69% decrease in the sHSP  $\alpha$ B-crystallin in the myometrium at labor plus multiple isoforms of HSP27. Immunoblotting using phosphospecific HSP27 antibodies (HSP27-serine15, -78, and -82) detected marked changes in HSP27 phosphorylation at

labor. Although total HSP27 levels were unchanged, HSP27-Ser15 was 3-fold higher at labor. Coimmunoprecipitation studies showed that HSP27 coprecipitates with  $\alpha$ B-crystallin and also smooth muscle  $\alpha$ -actin. Coimmunofluorescence studies demonstrated a relocation of HSP27 from the perinuclear region to the actin cytoskeleton at labor. The functional significance of these changes was demonstrated *in vitro* where myometrial strips stimulated to contract with oxytocin exhibited increased HSP27-Ser15 phosphorylation. Our findings provide data consistent with a novel pathway regulating human myometrial contraction at labor and identify HSP27 and  $\alpha$ B-crystallin as potential targets for future tocolytic design. (*Endocrinology* 149: 245–252, 2008)

A CRITICAL ASPECT of normal human birth is the ability of uterine smooth muscle (myometrium) to respond to contractile stimulants (uterotonics) and to produce coordinated, forceful contractions. This involves a significant remodeling process that includes increased connectivity (*e.g.* the formation of gap junctions) between myocytes and changes in myocyte excitability as well as major changes to the cytoskeleton (1, 2).

Myometrial contractility is considered to be regulated primarily by intracellular free calcium ion concentration ( $[Ca^{2+}]_i$ ). Increased  $[Ca^{2+}]_i$  results in enhanced interaction between calmodulin and myosin light chain kinase (MLCK). Phosphorylation of MLC triggers cross-bridge cycling along fibrillar actin filaments and the development of force necessary for contraction (1, 3). Relaxation of the muscle is thought to be a reversal of this process; that is, the removal of  $[Ca^{2+}]_i$  induces dissociation of calmodulin from MLCK. When myosin is dephosphorylated by MLC phosphatases, it dissociates from the actin filament, and relaxation occurs. Despite widespread acceptance of this model, discrepancies remain. Smooth muscle contraction can be sustained in the continued presence of a contractile agonist, although in-

creases in  $[Ca^{2+}]_i$  and MLC phosphorylation are transient (4, 5). This suggests that there are additional mechanisms involved in the regulation of smooth muscle contractility.

Changes in the cytoskeletal machinery of smooth muscle cells endow the cells with the structural and functional capacity to generate force and contract (6). The regulation of this process in the human myometrium is unknown, but data from other muscle cells suggest that small heat shock proteins (sHSP), such as  $\alpha$ B-crystallin and HSP27, play an important role.  $\alpha$ B-crystallin and HSP27 are highly expressed in muscle and can directly interact with each other to form homo-oligomers as well as hetero-oligomeric complexes (7–10). Furthermore, these proteins can interact with components of the actin cytoskeleton to modulate actin filament formation and thus contraction (11, 12). For example, HSP27 is a known actin-binding protein that can modulate actin filament dynamics through actin polymerization inhibition (13, 14). Additionally, overexpression of HSP27 in fibroblast cells promotes the accumulation of fibrillar actin (F-actin) (15).

The functional characteristics of sHSP are predominantly determined by phosphorylation, which induces a change in the tertiary structure of these proteins, thereby altering their affinity to form homo- or hetero-oligomers or to interact with the actin cytoskeleton. For example, phosphorylation induces the dissociation of  $\alpha$ B-crystallin (16) and HSP27 multimers (17, 18) into small monomer and dimer subunits. HSP27 has three predominant sites of phosphorylation, serine residues 15, 78, and 82 (19, 20). The substitution of these serine residues with glycine prevents the dissociation of HSP27 oligomers and prohibits HSP27-mediated accumulation of F-actin (21), thereby supporting a role for HSP27

First Published Online October 4, 2007

Abbreviations: Cy, Cyanine; 1D, one-dimensional; 2D-DIGE, two-dimensional difference gel electrophoresis; F-actin, fibrillar actin; HSA, human serum albumin; MALDI-ToF, matrix-assisted laser desorption/ionization time-of-flight; MLCK, myosin light chain kinase; NP40, Nonidet P-40; sHSP, small heat shock protein;  $\alpha$ -SMA,  $\alpha$ -smooth muscle actin; TBST, Tris-buffered saline supplemented with 0.01% Tween 20.

*Endocrinology* is published monthly by The Endocrine Society (<http://www.endo-society.org>), the foremost professional society serving the endocrine community.

phosphorylation in actin filament stabilization. Moreover, it has been proposed that the phosphorylation of HSP27 on serine residue 15 increases its propensity to bind to and stabilize actin filaments, in turn promoting contraction (11, 18).

In this study, we hypothesized that human labor onset is associated with changes in the abundance and posttranslational modification (e.g. phosphorylation) of key regulatory myometrial proteins. Specifically, we sought to characterize labor-associated changes in the sHSP  $\alpha$ B-crystallin and HSP27 in human myometrium.

## Materials and Methods

### Experimental subjects

All experimental procedures performed in this study were approved by the University of Newcastle Ethics Committee in accordance with the institutional guidelines of the John Hunter Hospital, Australia, and the KK Women's and Children's Hospital, Singapore. Informed consent was obtained from women before elective or emergency cesarean section. Myometrial tissue strips (5 × 10 mm) were sampled from the upper margins of the lower uterine segment, freed of connective tissue, immediately snap-frozen in liquid nitrogen, and either stored at –80 C or prepared for bioassay and stored in saline at 4 C for up to 16 h. All women undergoing cesarean section were examined clinically, and those exhibiting signs of infection were excluded. Women who chose elective cesarean section and showed no signs of labor (uterine contractions and/or cervical changes) formed the nonlaboring group. Women who entered spontaneous and established labor (at least 2 h) but required emergency cesarean section formed the laboring group. Clinical indications for emergency cesarean section included breech, fetal distress, prolonged labor, and previous cesarean section. All subjects were between 37 and 40 wk gestational age.

### Extraction of myometrial proteins and depletion of human serum albumin (HSA) and IgG

Myometrial tissue samples were crushed under liquid nitrogen and then homogenized in a urea/CHAPS-based lysis buffer (7 M urea, 2 M thiourea, 4% wt/vol 30 mM CHAPS, pH 8.5) at a ratio of 100 mg crushed tissue/1 ml extraction buffer. The homogenate was centrifuged (13,000 × g for 15 min at 4 C), and the resulting supernatant was collected. Depletion of HSA and IgG was performed using the albumin and IgG removal kit (GE Healthcare, Piscataway, NJ) according to the manufacturer's protocol. Briefly, extracts were incubated with an anti-HSA/anti-IgG resin for 30 min at room temperature. Unbound proteins were then separated from the absorption matrix using a mini-spin cartridge and centrifuging the sample at 1000 × g for 2 min. Concentration and desalting of HSA/IgG-depleted samples was performed by acetone precipitation. Four volumes of ice-cold acetone were added to each sample, incubated for 3 h at –20 C, and then centrifuged (13,000 × g for 15 min at 4 C). Samples were resuspended in 50  $\mu$ l extraction buffer. Protein concentration estimation was performed using the 2-D Quant Kit (GE Healthcare, Uppsala, Sweden).

### Fluorescent cyanine (Cy)-dye labeling of samples

Before labeling, Cy dyes Cy2, -3, and -5 (GE Healthcare) were reconstituted in anhydrous dimethylformamide. Nonlaboring (n = 6) or laboring (n = 6) myometrial proteins (50  $\mu$ g) were labeled with 400 pM of either Cy3 or Cy5 dye on ice for 30 min in the dark. To account for any dye binding bias, half of every sample group was labeled with Cy3, whereas the remaining half was labeled with Cy5. An internal pooled sample was created by mixing 25  $\mu$ g of each sample and labeling as above with Cy2. Dye labeling reactions were stopped with 10 mM lysine. Cy3- and Cy5-labeled samples were mixed with the Cy2-labeled pooled control and made up to 450  $\mu$ l with rehydration buffer (7 M urea, 2 M thiourea, 4% wt/vol CHAPS, 2 mg/ml dithiothreitol, and 1% vol/vol pH 3–10 immobilized pH gradient buffer).

### Two-dimensional difference gel electrophoresis (2D-DIGE)

In-gel rehydration of immobilized pH gradient strips (nonlinear, pH 3–10, 240 mm; GE Healthcare) was performed with the Cy-labeled samples overnight for 12 h at room temperature under mineral oil (Sigma Chemical Co., St. Louis, MO). Isoelectric focusing was performed using a Multiphor II unit (GE Healthcare) for a total of 58,800 Vh using the following parameters: hold at 300 V for 900 Vh, ramp and hold at 1000 V for 3900 Vh, ramp and hold to 8000 V for 13,000 Vh, and hold at 8000 V for 41,000 Vh. Strips were then equilibrated and reduced in equilibration buffer (30% vol/vol glycerol, 2% wt/vol SDS, 7 M urea, trace bromophenol blue) with 0.5% dithiothreitol for 15 min at room temperature and then in equilibration buffer containing 4.5% iodoacetamide for 15 min at room temperature. Strips were then placed on homogeneous 10% acrylamide gels (255 × 205 mm) cast in low-fluorescence plates using the Ettan DALTsix Electrophoresis Casting System (GE Healthcare). This produced six simultaneously cast gels using the same batch of acrylamide gel stock solution for each gel. Second-dimensional electrophoretic separation was carried out at 2.5 W/gel constant power for 30 min and then 100 W (total) constant power using a peltier-cooled Ettan DALT II electrophoresis unit (GE Healthcare) until the bromophenol dye front reached the bottom of the gel.

### Imaging and analysis of 2D-DIGE gels

Fluorescence image acquisition was performed using the Typhoon 9400 Variable Mode Imager (GE Healthcare). Each gel was scanned at the following excitation/emission wavelengths: 480/530nm (Cy2), 520/590nm (Cy3), and 620/680 nm (Cy5). Gel analysis was conducted using the DeCyder version 5.0 Biological Variation software module (GE Healthcare) for spot matching, quantitation, and standardization of protein spot data. Spot matching was validated by manual inspection of gel spots. Statistically significant protein abundance changes were identified via Student's *t* test. Proteins present in either all gels or at least in all nonlaboring or laboring gels and whose abundance changed more than 1.5-fold (*P* < 0.05) were chosen as proteins for identification.

### Matrix-assisted laser desorption/ionization time-of-flight (MALDI-ToF) protein sequencing

A preparative sequencing gel was prepared by performing 2D-PAGE on 500  $\mu$ g of pooled myometrium proteins. The gel was fixed in 50% methanol/7% acetic acid for 30 min and then stained with SYPRO Ruby (Invitrogen, Carlsbad, CA) overnight at room temperature. The gel was then washed in 10% methanol/7% acetic acid, briefly rinsed in distilled water, and visualized using a UV transilluminator. Target proteins were excised and destained in 50 mM ammonium bicarbonate in 50% vol/vol methanol for three washes of 40 min each. Gel plugs were dried at 37 C for 2 h and then incubated in 40 ng/ $\mu$ l trypsin (Promega, Madison, WI) in 20 mM ammonium bicarbonate at 37 C for 3 h. Sequencing was performed using an Ettan MALDI-ToF Pro (GE Healthcare). For this, 1  $\mu$ l tryptic peptide was mixed with 1  $\mu$ l  $\alpha$ -cyano-4-hydroxycinnamic acid matrix (5 mg/ml in 50% acetonitrile, 0.1% trifluoroacetic acid), and 1  $\mu$ l of this mixture was spotted in duplicate onto the MALDI target tray. Peptide mass fingerprinting was performed alongside peptide standards in reflectron mode. Sequence data were used to interrogate the Swiss-Prot and NCBI nr databases. As an additional control measure, the isoelectric point and molecular weight of identified proteins were checked against the region of the pick gel from which they were excised.

### One-dimensional (1D) SDS-PAGE and immunoblotting

Myometrial proteins (10  $\mu$ g) were loaded on precast 12% NuPAGE acrylamide gels (Invitrogen) and separated electrophoretically using the Xcell SureLock Mini-Cell system at 190 V (constant) until the bromophenol blue dye migrated to the bottom of the gel. Proteins were then transferred to nitrocellulose (Hybond C; GE Healthcare) using the Xcell II blot module (Invitrogen) at 30 V for 55 min. Membranes were blocked with 5% skim milk in Tris-buffered saline supplemented with 0.01% Tween 20 (TBST) for 2 h and then incubated with antibodies for  $\alpha$ B-crystallin (1:3000; Stressgen Bioreagents, Victoria, Canada), total HSP27 (1:2500), pHSP27-Ser15 (1:1000), pHSP27-Ser78 (1:2000), and pHSP27-Ser82 (1:2000) in 5% skim milk/TBST for 2 h at room temperature. HSP20

and HSP27 antibodies were purchased from Upstate Biotechnology (Lake Placid, NY). Membranes were then washed five times (5 min per wash) in TBST, and the appropriate secondary antibody (1:2000) was added for 1 h at room temperature. Immunoreactive protein was detected with enhanced chemiluminescence (GE Healthcare) using the Intelligent Dark Box LAS-3000 Imager (Fuji Photo Film, Tokyo, Japan). Membranes were stripped with 0.2 M NaOH and then reprobed with  $\alpha$ -smooth muscle actin ( $\alpha$ -SMA, 1:2000; Sigma) as a loading control.  $\alpha$ -SMA abundance of actin protein in human myometrium remains unchanged with and during pregnancy (22, 23). Similarly, in rat myometrium,  $\alpha$ -SMA mRNA and protein levels remain unchanged throughout gestation and labor onset (24). HSP27 phosphorylation was also standardized to  $\alpha$ -SMA because its relative molecular mass ( $M_r \sim 42 \times 10^3$ ) differs from that of HSP27 and its phospho-forms ( $M_r \sim 27 \times 10^3$ ). Thus, we were able to avoid any issues of inhibited interaction between the antibody and the ligand during reprobing caused by residual HSP27 phospho-antibody binding. Specificity of immunoreactive bands was assessed by probing with preimmune antisera followed by secondary antibody and also secondary antibody alone. Densitometric analysis was performed using Multi-Gauge (Fuji Photo Film) image analysis software. Band intensity values of  $\alpha$ B-crystallin and HSP27 were standardized to those of  $\alpha$ -SMA. Statistical analysis was performed with GraphPad InStat version 3.0 (GraphPad Software, San Diego, CA).

### Coimmunoprecipitation

Myometrial proteins (~100 mg,  $n = 5$  for both nonlaboring and laboring samples) were extracted in 1 ml Nonidet P-40 (NP40) lysis buffer (150 mM NaCl, 50 mM Tris-HCl, 5 mM EDTA, 0.5% NP40). One microgram of rabbit-anti-HSP27 antibody (Upstate Biotechnology) was added to 50  $\mu$ g extracted protein. As a control, 1  $\mu$ g normal rabbit IgG was added to 50  $\mu$ g pooled nonlaboring and laboring myometrial protein extracts. The protein-antibody mixture was incubated overnight at 4 C, and then 20  $\mu$ l protein A-agarose immunoprecipitation reagent was added and incubated for 1 h at 4 C. The mixture was centrifuged at  $1000 \times g$  for 5 min at 4 C, and the resulting pellet was washed three times for 5 min each with 1 ml NP40 lysis buffer. The pellet was resuspended in 60  $\mu$ l  $1 \times$  lithium dodecyl sulfate buffer (Invitrogen) and heated at 70 C for 10 min. Samples were then centrifuged at  $12,000 \times g$  for 10 min and the supernatant collected. Immunoprecipitated protein (20  $\mu$ l) was resolved by 1D SDS-PAGE, transferred to nitrocellulose, and probed with antibodies for  $\alpha$ B-crystallin, HSP27, and  $\alpha$ -SMA.

### Immunofluorescence microscopy and colocalization analysis

Myometrial tissue obtained at cesarean section ( $n = 6$  for nonlaboring and laboring) were immediately fixed in neutral-buffered formalin for 48 h and embedded in paraffin. Sections of 10  $\mu$ m were attached to low-fluorescence glass slides. Slides were deparaffinized by incubating in the following solutions for 5 min each:  $2 \times 100\%$  xylene,  $3 \times 100\%$  absolute alcohol, 80% ethanol, and 70% ethanol. Antigen retrieval was performed by microwave heating the slides in citrate buffer (pH 6) at 95 C. Sections were blocked in 10% fetal calf serum in PBS for 30 min and then incubated in  $\alpha$ B-crystallin (1:400), HSP27 (1:400) and  $\alpha$ -SMA (Sigma, 1:500) antibodies diluted in 10% fetal calf serum. Alexa Fluor 488 goat antimouse IgG and Alexa Fluor 594 goat antirabbit IgG (Invitrogen; both 1:2000) were used as secondary antibodies. 4',6-Diamidino-2-phenylindole (300 nm) was used as a nuclear stain. As controls, sections were incubated with preimmune sera and/or secondary antibodies alone. Only specimens demonstrating low background with control staining were used for analysis. Slides were mounted for imaging by adding 15  $\mu$ l Vectorshield H-1000 (Invitrogen) mounting media. Immunofluorescence microscopy was performed using a Zeiss Axiocam MRm(v2) and Axioplan 2 epifluorescent microscope (Carl Zeiss, Sydney, Australia). Specimens were visualized using band pass filter sets that demonstrate negligible spectral overlap. Image registration in each channel was calibrated using a Focalcheck fluorescence microscope test slide (no. 1; Molecular Probes, Invitrogen). For each patient pair, nonsaturated images were collected with identical microscope and camera settings using the Axiovision software package (version 4.4). Colocalization analyses were then performed using the Colocalization Module of the software that creates a scatterplot of each channel. Defining a threshold creates

a colocalization mask to represent high-intensity green and red pixels. The same threshold values were used for each sample pair comparison.

### Isometric tension recordings

Myometrial samples were dissected into strips ( $7 \times 2 \times 2$  mm), connected to a Grass FT03C force transducer (Grass Instruments, Quincy, MA), and suspended in organ baths containing 15 ml Krebs' physiological salt solution. Strips were maintained at 37 C and pH 7.4 and continuously gassed with 95% O<sub>2</sub>/5% CO<sub>2</sub>. Passive tension of 1 mN was applied to each strip, and strips were allowed to equilibrate for 60–90 min until the development of spontaneous regular contractions. Strips were then exposed to a single dose of oxytocin  $10^{-7}$  M for 5–20 min (until maximal tension reached) and immediately frozen in liquid nitrogen. Contractility was measured by integrating the area under the tension curve, using a MacLab 8E data acquisition system with Chart software (version 5; ADI, Melbourne, Australia). Responses to oxytocin were compared as a percentage of spontaneous activity before treatment. Total and phosphorylated HSP27 was assessed using immunoblotting as previously described.

## Results

Protein profiles of term nonlaboring human myometria ( $n = 6$ ) and term spontaneously laboring myometria ( $n = 6$ ) were quantitatively compared using 2D-DIGE (25) (Fig. 1A). One of the most prominent changes detected in protein abundance was a 69% decrease (Student's *t* test,  $P < 0.05$ ) in the sHSP  $\alpha$ B-crystallin (accession no. P02511) in laboring myometria (Fig. 1B and Table 1). Consistent with these results, immunoblotting for  $\alpha$ B-crystallin in a larger sample cohort showed a 71% decrease (Mann-Whitney *U* test,  $P < 0.01$ ) in laboring myometria ( $n = 11$ ) compared with nonlaboring tissue ( $n = 13$ ) (Fig. 1D). The 2D-DIGE study also identified three isoforms of HSP27 (accession no. P04792) resolved in the form of a charge-train, indicative of posttranslational modification (Fig. 1C and Table 1).

To determine whether  $\alpha$ B-crystallin and HSP27 interact as reported for other tissues (7, 10), coimmunoprecipitation was employed. HSP27 immunoprecipitates from nonlaboring ( $n = 5$ ) and laboring myometria ( $n = 5$ ) were resolved by 1D SDS-PAGE, transferred to nitrocellulose, and probed with antibodies for HSP27 and  $\alpha$ B-crystallin (Fig. 2A). A single band of approximate relative molecular mass ( $M_r$ ) of  $23 \times 10^3$  corresponding to  $\alpha$ B-crystallin was detected in nonlaboring and, to a lesser extent, laboring myometria. In contrast, no band was detected in the negative control (preimmune rabbit IgG), suggesting specific association between  $\alpha$ B-crystallin and HSP27 in these samples. Because HSP27 is a known actin-binding protein that may mediate smooth muscle contraction through stabilization of the actin filaments, we also probed the HSP27 immunoprecipitates for  $\alpha$ -SMA (Fig. 2A). A positive immunoreaction was observed in both nonlaboring and laboring myometria, indicating specific interactions between HSP27 and actin in the human myometrium at the time of labor.

Coimmunofluorescence was then performed to examine the cellular localization of  $\alpha$ B-crystallin, HSP27, and  $\alpha$ -SMA in the myometrium at labor. In nonlaboring myometria,  $\alpha$ B-crystallin was primarily localized to the perinuclear region (Fig. 2B). A similar pattern of staining was observed for HSP27. By applying a colocalization algorithm that identifies regions of costaining, high levels of colocalization between  $\alpha$ B-crystallin and HSP27 were demonstrated in the both the perinuclear and cytoplasmic regions of nonlaboring myocytes. This result is consistent with

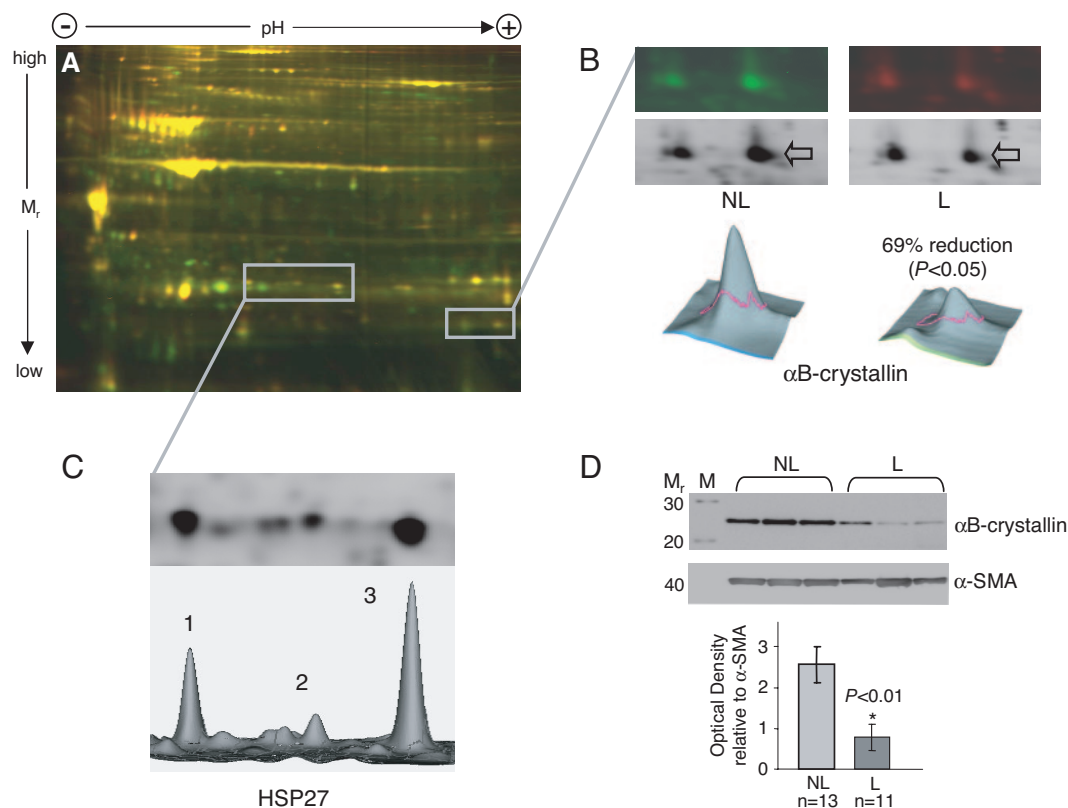


FIG. 1. 2D-DIGE analysis of human myometrium at labor onset. A, Representative 2D-DIGE gel showing comparison between protein profiles of nonlaboring myometrium (Cy3, green) and laboring myometrium (Cy5, red). Proteins were extracted from nonlaboring (NL,  $n = 6$ ) and laboring (L,  $n = 6$ ) myometrial biopsies and quantitatively compared using 2D-DIGE. B, One of the most marked changes in human myometrium after labor onset was a 69% decrease ( $P < 0.05$ , Student's  $t$  test) in the sHSP  $\alpha$ B-crystallin (arrows), as identified using MALDI-ToF mass spectrometry. C, 2D-DIGE combined with MALDI-ToF mass spectrometry also identified three (numbered 1, 2, and 3) highly abundant isoforms of HSP27. D, Representative immunoblot of  $\alpha$ B-crystallin in nonlaboring (NL,  $n = 13$ ) and laboring (L,  $n = 11$ ) myometria. Densitometric analysis of band intensity showed a significant 71% decrease ( $P < 0.01$ ) in the abundance of  $\alpha$ B-crystallin in laboring myometria. Quantitation of  $\alpha$ B-crystallin immunoreactive bands was performed by standardizing to the band intensity of  $\alpha$ -SMA.  $M_r$ , Relative molecular mass  $\times 1000$ ; M, molecular weight marker.

the coimmunoprecipitation of these two proteins. This relationship was completely different in laboring samples where HSP27 was detected in a fibrillar arrangement throughout the perinuclear and cytoplasmic regions, which was highly colocalized with  $\alpha$ -SMA (Fig. 2C). In these tissues,  $\alpha$ B-crystallin was barely detectable above background levels.

Phosphorylation of HSP27 has been shown to promote the dissociation of sHSP oligomeric complexes (7, 9) and modulate the ability of HSP27 to interact with actin (11, 18). We hypothesized that changes in the relocation of HSP27 to the actin cytoskeleton in the myometrium during labor are associated with changes in its phosphorylation status. Immunoblotting with phosphospecific antibodies (HSP27-Ser15, -78, and -82) revealed marked changes in HSP27 phosphorylation at labor

relative to  $\alpha$ -SMA (Fig. 3A). Although total abundance of HSP27 was unchanged, HSP27-Ser15 was 3.0-fold higher in laboring myometria (Mann-Whitney  $U$  test,  $P < 0.05$ ; Fig. 3B). In contrast, levels of HSP27-Ser82 were 85% less in laboring myometria (Mann-Whitney  $U$  test,  $P < 0.01$ ). There was no significant change in HSP27-Ser78.

To confirm that the changes in HSP27 were related to contractile events, phosphorylation of HSP27 was also measured *in vitro* after treatment of nonlaboring myometrial strips with the uterotonic oxytocin (Fig. 4). Oxytocin treatment showed an average  $206 \pm 64\%$  (mean  $\pm$  SEM,  $n = 5$ ) increase in contractility above baseline. This was associated with a significant increase in HSP27-Ser15 phosphorylation compared with matched controls (paired Student's  $t$  test,  $P < 0.05$ ; Fig. 4, B and C). Phos-

TABLE 1. MALDI-ToF mass spectrometry identification of sHSP in human myometrium

Protein ID	Swiss-Prot accession no.	Peptides matched (% coverage)	Theoretical/observed $M_r$	Theoretical/observed pI
$\alpha$ B-crystallin	P02511	3(14.3%)	20.14/~23	6.8/~8
HSP27 spot 1	P04792	5(26.3%)	22.76/~27	6/~6
HSP27 spot 2	P04792	7(48.8%)	22.76/~27	6/~6.1
HSP27 spot 3	P04792	7(46.5%)	22.76/~27	6/~6.4

Proteins were excised from preparative sequence gels, trypsinized, and sequenced using MALDI-ToF mass spectrometry. The observed isoelectric point (pI) and relative molecular mass ( $M_r \times 10^3$ ) of sequenced proteins were compared with theoretical values.

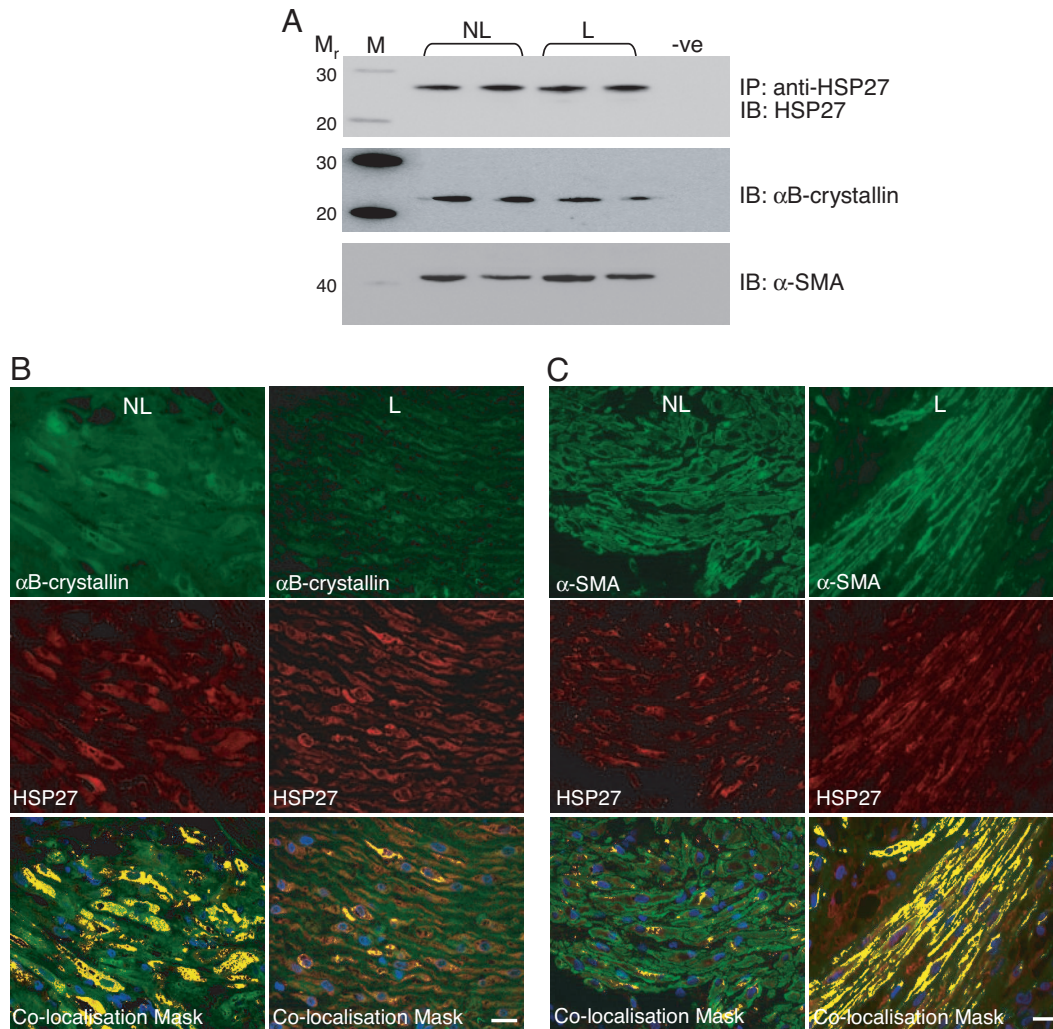


FIG. 2. Interaction of HSP27 with  $\alpha$ B-crystallin and  $\alpha$ -SMA in nonlaboring (NL) and laboring (L) myometria. A, Myometrial protein extracts immunoprecipitated (IP) with rabbit anti-HSP27 antibody were resolved by 1D SDS-PAGE and transferred to nitrocellulose. Immunoblotting (IB) was then performed using antibodies for HSP27,  $\alpha$ B-crystallin, and  $\alpha$ -SMA. As a negative control (-ve), IP was also performed using preimmune rabbit IgG. Associations between HSP27 and  $\alpha$ B-crystallin, and HSP27 and  $\alpha$ -SMA, were observed in both nonlaboring and laboring myometria ( $n = 5$  for both groups). B and C, Colocalization of HSP27 with  $\alpha$ B-crystallin (B) and HSP27 with  $\alpha$ -SMA (C) in nonlaboring (NL,  $n = 5$ ) and laboring (L,  $n = 5$ ) myometria. Colocalization masks that highlight regions of costaining (yellow) were generated as described in *Materials and Methods*. High levels of colocalization between HSP27 and  $\alpha$ B-crystallin were observed in the perinuclear and cytoplasmic region of nonlaboring myometria. This relationship was lost with the onset of labor. In nonlaboring myometria, low levels of colocalization between HSP27 and  $\alpha$ -SMA were observed. In contrast, HSP27 and  $\alpha$ -SMA showed high levels of colocalization in laboring tissues particularly along F-actin bundles. Scale bar, 20  $\mu$ M.  $M_r$ , Relative molecular mass  $\times 1000$ ; M, molecular weight marker.

phorylation of HSP27-Ser78 and -Ser82 did not alter with oxytocin treatment.

### Discussion

We describe for the first time in the human myometrium labor-associated changes in the sHSP  $\alpha$ B-crystallin and HSP27. We provide evidence that changes in these proteins are associated with actin cytoskeletal remodeling at the time of labor and use *in vitro* stimulation of myometrial muscle strips to show these changes are directly related to contraction.

As revealed using 2D-DIGE, one of the most significant changes in protein abundance in the human myometrium at labor is a 69% decrease in  $\alpha$ B-crystallin (Fig. 1A). Corroborative evidence was provided using immunoblotting in a larger sample population

(Fig. 1B). Scant information exists regarding the function and regulation of  $\alpha$ B-crystallin in smooth muscle; however, in skeletal muscle,  $\alpha$ B-crystallin acts as a chaperone protein providing cells with cytoprotection during stress by preventing protein aggregation (26). Evidence suggests  $\alpha$ B-crystallin may also be important in the regulation of intermediate filaments (27–29). Mutations in the  $\alpha$ B-crystallin gene lead to the breakdown and aggregation of intermediate filaments and the development of skeletal and cardiomyopathies (30–32). Decreased levels of  $\alpha$ B-crystallin in actively contracting myometria are not consistent with such observations and suggest the protein may have a different function in myometrial smooth muscle.

Specific interactions between  $\alpha$ B-crystallin and HSP27 have previously been reported in muscle cells (33). We found that

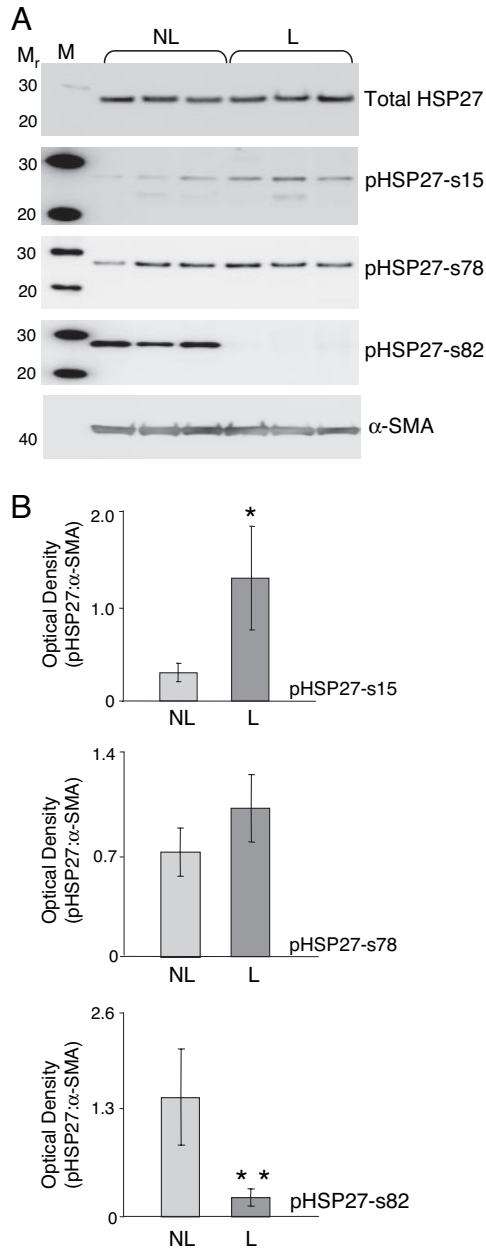


FIG. 3. Immunoblot analysis of total and phosphorylated forms of HSP27 in nonlaboring (NL) and laboring (L) myometria. A, Representative immunoblots demonstrating the abundance of total and phosphorylated forms of HSP27 (pHSP27-Ser15, pHSP27-Ser78, and pHSP27-Ser82) in nonlaboring (NL,  $n = 13$ ) and laboring (L,  $n = 11$ ) myometrium. B, Densitometric analysis of band intensity revealed that pHSP27-Ser15 was 3-fold higher (\*,  $P < 0.05$ , Mann-Whitney  $U$  test) in laboring myometria. In contrast, pHSP27-Ser82 abundance was decreased 84.62% (\*\*,  $P < 0.01$ , Mann-Whitney  $U$  test) in laboring samples. Abundance of pHSP27-Ser78 remained unchanged with labor. Quantitation of HSP27 immunoreactive bands was performed by standardizing to the band intensity of  $\alpha$ -SMA.  $M_r$ , Relative molecular mass  $\times 1000$ ; M, molecular weight marker.

these proteins interact primarily in the cytoplasm of nonlaboring myometria (Fig. 2, A and B). Most likely due to decreased levels of  $\alpha$ B-crystallin, this interaction is almost completely lost with labor (Fig. 2C). The functional significance of  $\alpha$ B-crystallin/HSP27 complexes in human myometria is unclear; how-

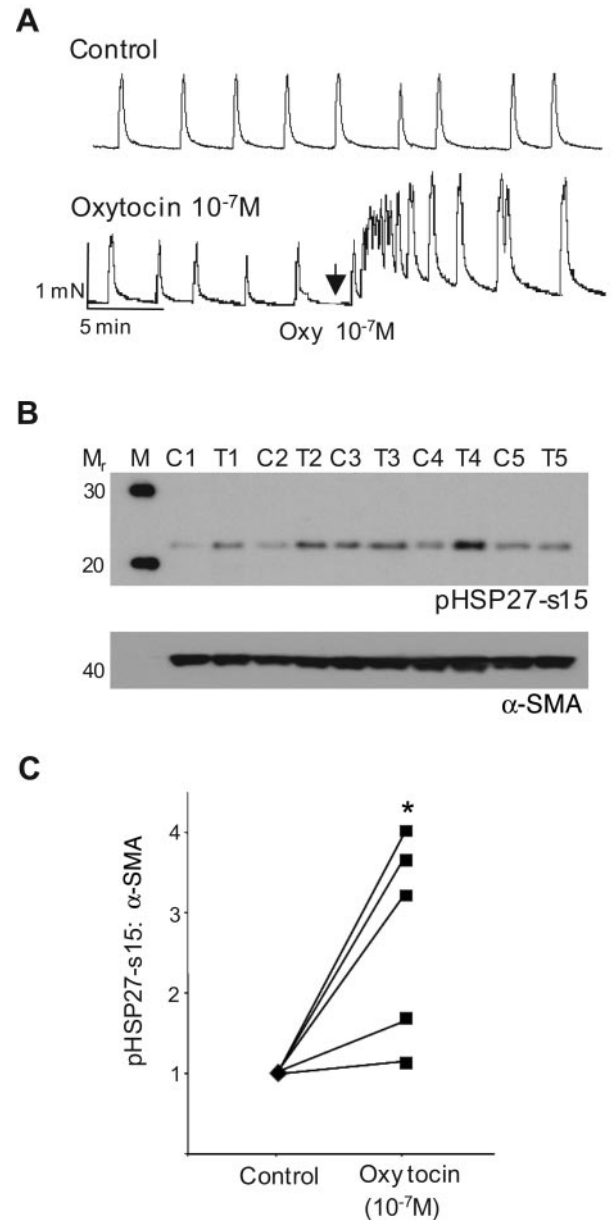


FIG. 4. Changes in phosphorylation of HSP27 in oxytocin-stimulated contractions in nonlaboring myometrial strips. A, Representative tracing of spontaneous and oxytocin-stimulated contractions in nonlaboring myometrium. There was an increase in contractility of  $206 \pm 64\%$  (mean  $\pm$  SEM,  $n = 5$ ) above baseline values. B, Immunoblotting of pHSP27-Ser15 abundance in control (C) and matched oxytocin-treated (T) myometrial muscle strips. C, Densitometric analysis of the immunoblots revealed a significant 2.7-fold increase ( $P < 0.05$ ) in pHSP27-Ser15 after oxytocin treatment. Band intensity of pHSP27-Ser15 was standardized to the band intensity of  $\alpha$ -SMA.  $M_r$ , Relative molecular mass  $\times 1000$ ; M, Molecular weight marker.

ever, we propose that decreased expression of  $\alpha$ B-crystallin at the time of labor liberates HSP27 enabling it to participate in other cellular events such as cytoskeletal remodeling.

HSP27 can modulate cytoskeletal dynamics through the F-actin stabilization and microfilament organization (11, 29, 34). Phosphorylation of HSP27 in human platelets increases F-actin formation (35), whereas HSP27 phosphorylation is required for growth factor stimulation of F-actin formation in cultured cells

(15, 21). This suggests HSP27-actin interaction is modulated by phosphorylation. Consistent with a role in actin remodeling, we found that HSP27 is relocated from the cytoplasm of nonlaboring myometria, where it is associated with  $\alpha$ B-crystallin, to the actin cytoskeleton in laboring myometria (Fig. 2, B and C). Moreover, we observed that this relocation occurs simultaneously with increased HSP27-Ser15 phosphorylation and concurrent HSP27-Ser82 dephosphorylation at labor. Similar results have been reported by in the rat myometrium where HSP27-Ser15 phosphorylation is increased at the end of pregnancy (36). HSP27-Ser15 phosphorylation is thought to facilitate binding to and subsequent stabilization of actin filaments (18), a notion consistent with increased HSP27-Ser15 phosphorylation at labor. The significance of HSP27-Ser82 dephosphorylation in the myometrium is unknown but it is plausible that such a modification would confer a conformational change upon the protein, potentially modulating its interaction with other sHSP and/or components of the actin cytoskeleton.

*In vitro* treatment of nonlaboring myometrial muscle strips with the uterotonic oxytocin increased contractility 206% above baseline (Fig. 4A). These samples exhibited significantly higher levels of HSP27-Ser15 phosphorylation, confirming the association between HSP27-Ser15 phosphorylation and myometrial contraction. It has previously been reported that stimulation of rat aortic vascular muscle contraction with angiotensin II induces HSP27 phosphorylation (37). Likewise, the vasoconstrictor thrombin increases HSP27 phosphorylation in both mouse cardiac myocytes (38) and aortic smooth muscle cells (39). Typically, these agonists have been shown to induce HSP27 phosphorylation via signal transduction cascades involving either p38 MAPK and its downstream targets MAPK-activated protein kinase-2 and -3 (37, 40, 41) or through protein kinase C activation (42). Consistent with a proposed role in smooth muscle contraction, the inhibition of HSP27 phosphorylation in rat aorta smooth muscle cells inhibits angiotensin II-induced contraction (37). Therefore, the evidence supports a critical role for HSP27 phosphorylation in myometrial contraction.

Our results support the hypothesis that smooth muscle contraction is more than the regulation of intracellular  $Ca^{2+}$  concentrations and the regulation of MLCK activity by second messenger systems. Our findings suggest that modulation of actin cytoskeletal assembly by sHSP may be an important additional regulated step. This new knowledge could have important consequences as the pathways regulating the phosphorylation and synthesis of sHSP are uncovered in different tissues. In the myometrium, it seems that an old uterotonic oxytocin may have a new modus operandi as a regulator of HSP27 phosphorylation.

### Acknowledgments

We thank T. Engel, T. Finnegan, and the staff of the Obstetrics and Gynaecology Divisions at the John Hunter Hospital, Newcastle, Australia, and KK Children's and Women's Hospital, Singapore, for patient recruitment and sample collection. We also acknowledge R. F. Thorne from the Cancer Research Unit at the University of Newcastle, New South Wales, Australia, for materials and advice regarding immunofluorescence.

Received May 21, 2007. Accepted September 25, 2007.

Address all correspondence and requests for reprints to: Dr. Eng-Cheng Chan, Mothers and Babies Research Centre, The University of Newcastle,

John Hunter Hospital, 1 Lookout Road, New Lambton Heights, Newcastle 2305, Australia. E-mail: Cheng.Chan@newcastle.edu.au.

Disclosure Statement: The authors of this manuscript have nothing to declare.

### References

- Sanborn BM, Ku CY, Shlykov S, Babich L 2005 Molecular signaling through G-protein-coupled receptors and the control of intracellular calcium in myometrium. *J Soc Gynecol Investig* 12:479–487
- Smith R 2007 Mechanisms of disease: parturition. *N Engl J Med* 356:271–283
- Lopez Bernal A 2003 Mechanisms of labour: biochemical aspects. *BJOG* 110(Suppl 20):39–45
- Gerthoffer WT 1987 Dissociation of myosin phosphorylation and active tension during muscarinic stimulation of tracheal smooth muscle. *J Pharmacol Exp Ther* 240:8–15
- Woodrum DA, Brophy CM 2001 The paradox of smooth muscle physiology. *Mol Cell Endocrinol* 177:135–143
- Mehta D, Gunst SJ 1999 Actin polymerization stimulated by contractile activation regulates force development in canine tracheal smooth muscle. *J Physiol* 519(Pt 3):829–840
- Zantema A, Verlaan-De Vries M, Maasdam D, Bol S, van der Eb A 1992 Heat shock protein 27 and  $\alpha$ B-crystallin can form a complex, which dissociates by heat shock. *J Biol Chem* 267:12936–12941
- Merck KB, Groenen PJ, Voorter CE, de Haard Hoekman WA, Horwitz J, Bloemendal H, de Jong WW 1993 Structural and functional similarities of bovine  $\alpha$ -crystallin and mouse small heat-shock protein. A family of chaperones. *J Biol Chem* 268:1046–1052
- Liu C, Welsh MJ 1999 Identification of a site of Hsp27 binding with Hsp27 and  $\alpha$ B-crystallin as indicated by the yeast two-hybrid system. *Biochem Biophys Res Commun* 255:256–261
- Fontaine JM, Sun X, Benndorf R, Welsh MJ 2005 Interactions of HSP22 (HSPB8) with HSP20,  $\alpha$ B-crystallin, and HSPB3. *Biochem Biophys Res Commun* 337:1006–1011
- Gerthoffer WT, Gunst SJ 2001 Invited review: focal adhesion and small heat shock proteins in the regulation of actin remodeling and contractility in smooth muscle. *J Appl Physiol* 91:963–972
- Gusev NB, Bogatcheva NV, Marston SB 2002 Structure and properties of small heat shock proteins (sHsp) and their interaction with cytoskeleton proteins. *Biochemistry (Mosc)* 67:511–519
- Miron T, Wilchek M, Geiger B 1988 Characterization of an inhibitor of actin polymerization in vinculin-rich fraction of turkey gizzard smooth muscle. *Eur J Biochem* 178:543–553
- Miron T, Vancompernelle K, Vandekerckhove J, Wilchek M, Geiger B 1991 A 25-kD inhibitor of actin polymerization is a low molecular mass heat shock protein. *J Cell Biol* 114:255–261
- Lavoie JN, Gingras-Breton G, Tanguay RM, Landry J 1993 Induction of Chinese hamster HSP27 gene expression in mouse cells confers resistance to heat shock. HSP27 stabilization of the microfilament organization. *J Biol Chem* 268:3420–3429
- Ito H, Kamei K, Iwamoto I, Inaguma Y, Nohara D, Kato K 2001 Phosphorylation-induced change of the oligomerization state of  $\alpha$ B-crystallin. *J Biol Chem* 276:5346–5352
- Mehlen P, Arrigo AP 1994 The serum-induced phosphorylation of mammalian hsp27 correlates with changes in its intracellular localization and levels of oligomerization. *Eur J Biochem* 221:327–334
- Lambert H, Charette SJ, Bernier AF, Guimond A, Landry J 1999 HSP27 multimerization mediated by phosphorylation-sensitive intermolecular interactions at the amino terminus. *J Biol Chem* 274:9378–9385
- Landry J, Lambert H, Zhou M, Lavoie JN, Hickey E, Weber LA, Anderson CW 1992 Human HSP27 is phosphorylated at serines 78 and 82 by heat shock and mitogen-activated kinases that recognize the same amino acid motif as S6 kinase 11. *J Biol Chem* 267:794–803
- Stokoe D, Engel K, Campbell DG, Cohen P, Gaestel M 1992 Identification of MAPKAP kinase 2 as a major enzyme responsible for the phosphorylation of the small mammalian heat shock proteins. *FEBS Lett* 313:307–313
- Lavoie JN, Hickey E, Weber LA, Landry J 1993 Modulation of actin microfilament dynamics and fluid phase pinocytosis by phosphorylation of heat shock protein 27. *J Biol Chem* 268:24210–24214
- Ewoane C, Cavaille F 1990 Interaction of actin from pregnant and nonpregnant human uterus with the uterine myosin subfragment-1: actin activated ATPase activities and actin binding. *Biochem (Life Sci Adv)* 9:71–77
- Word RA, Stull JT, Casey ML, Kamm KE 1993 Contractile elements and myosin light chain phosphorylation in myometrial tissue from nonpregnant and pregnant women. *J Clin Invest* 92:29–37
- Shynlova O, Tsui P, Doringin A, Chow M, Lye SJ 2005 Expression and localization of  $\alpha$ -smooth muscle and  $\gamma$ -actins in the pregnant rat myometrium. *Biol Reprod* 73:773–780
- Unlu M, Morgan ME, Minden JS 1997 Difference gel electrophoresis: a single gel method for detecting changes in protein extracts. *Electrophoresis* 18:2071–2077

26. Chavez Zobel AT, Loranger A, Marceau N, Theriault JR, Lambert H, Landry J 2003 Distinct chaperone mechanisms can delay the formation of aggresomes by the myopathy-causing R120G  $\alpha$ B-crystallin mutant. *Hum Mol Genet* 12:1609–1620
27. Nicholl ID, Quinlan RA 1994 Chaperone activity of  $\alpha$ -crystallins modulates intermediate filament assembly. *EMBO J* 13:945–953
28. Iwaki T, Kume-Iwaki A, Liem RK, Goldman JE 1989  $\alpha$ B-crystallin is expressed in non-lenticular tissues and accumulates in Alexander's disease brain. *Cell* 57:71–78
29. Perng MD, Cairns L, van den IP, Prescott A, Hutcheson AM, Quinlan RA 1999 Intermediate filament interactions can be altered by HSP27 and  $\alpha$ B-crystallin. *J Cell Sci* 112(Pt 13):2099–2112
30. Goldfarb LG, Park K, Cervenáková L, Gorokhova S, Lee H, Vasconcelos O, Nagle JW, Semino-Mora C, Sivakumar K, Dalakas MC 1998 Missense mutations in desmin associated with familial cardiac and skeletal myopathy. *Nat Genet* 19:402–403
31. Quinlan R, van den Ijssel PR 1999 Fatal attraction: when chaperone turns harlot. *Nat Med* 5:25–26
32. Vicart P, Caron A, Guicheney P, Li Z, Prevost MC, Faure A, Chateau D, Chapon F, Tome F, Dupret JM, Paulin D, Fardeau M 1998 A missense mutation in the  $\alpha$ B-crystallin chaperone gene causes a desmin-related myopathy. *Nat Genet* 20:92–95
33. Sugiyama Y, Suzuki A, Kishikawa M, Akutsu R, Hirose T, Wayne MM, Tsui SK, Yoshida S, Ohno S 2000 Muscle develops a specific form of small heat shock protein complex composed of MKBP/HSPB2 and HSPB3 during myogenic differentiation. *J Biol Chem* 275:1095–1104
34. Quinlan R 2002 Cytoskeletal competence requires protein chaperones. *Prog Mol Subcell Biol* 28:219–233
35. Butt E, Immler D, Meyer HE, Kotlyarov A, Laass K, Gaestel M 2001 Heat shock protein 27 is a substrate of cGMP-dependent protein kinase in intact human platelets. Phosphorylation-induced actin polymerization caused by Hsp27 mutants. *J Biol Chem* 276:7108–7113
36. White BG, Williams SJ, Highmore K, Macphee DJ 2005 Small heat shock protein 27 (Hsp27) expression is highly induced in rat myometrium during late pregnancy and labour. *Reproduction* 129:115–126
37. Meloche S, Landry J, Huot J, Houle F, Marceau F, Giasson E 2000 p38 MAP kinase pathway regulates angiotensin II-induced contraction of rat vascular smooth muscle. *Am J Physiol Heart Circ Physiol* 279:H741–H751
38. Tanabe K, Akamatsu S, Suga H, Takai S, Kato K, Dohi S, Kozawa O 2005 Midazolam suppresses thrombin-induced heat shock protein 27 phosphorylation through inhibition of p38 mitogen-activated protein kinase in cardiac myocytes. *J Cell Biochem* 96:56–64
39. Hirade K, Kozawa O, Tanabe K, Niwa M, Matsuno H, Oiso Y, Akamatsu S, Ito H, Kato K, Katagiri Y, Uematsu T 2002 Thrombin stimulates dissociation and induction of HSP27 via p38 MAPK in vascular smooth muscle cells. *Am J Physiol Heart Circ Physiol* 283:H941–H948
40. Larsen JK, Yamboliev IA, Weber LA, Gerthoffer WT 1997 Phosphorylation of the 27-kDa heat shock protein via p38 MAP kinase and MAPKAP kinase in smooth muscle. *Am J Physiol Lung Cell Mol Physiol* 273:L930–L940
41. Brophy CM, Woodrum D, Dickinson M, Beall A 1998 Thrombin activates MAPKAP2 kinase in vascular smooth muscle. *J Vasc Surg* 27:963–969
42. Bitar KN, Hillemeier C, Biancani P, Balazovich KJ 1991 Regulation of smooth muscle contraction in rabbit internal anal sphincter by protein kinase C and Ins(1,4,5)P<sub>3</sub>. *Am J Physiol* 260:G537–G542

*Endocrinology* is published monthly by The Endocrine Society (<http://www.endo-society.org>), the foremost professional society serving the endocrine community.